Hindawi
Journal of Sensors
Volume 2018, Article ID 3437149, 9 pages
https://doi.org/10.1155/2018/3437149

Research Article

A Molecularly Imprinted Electrochemical Gas Sensor to Sense Butylated Hydroxytoluene in Air

Shadi Emam,[1] **Adedokun Adedoyin**,[2] **Xiaohua Geng**,[2] **Mohsen Zaeimbashi**,[1] **Jason Adams**,[1] **Adam Ekenseair**,[2] **Elizabeth Podlaha-Murphy**,[3] **and Nian Xiang Sun**[1]

[1]*Department of Electrical Engineering, Northeastern University, Boston MA, USA*
[2]*Department of Chemical Engineering, Northeastern University, Boston MA, USA*
[3]*Department of Chemical and Biomolecular Engineering, Clarkson University, Potsdam NY, USA*

Correspondence should be addressed to Nian Xiang Sun; n.sun@northeastern.edu

Received 2 November 2017; Revised 19 February 2018; Accepted 1 April 2018; Published 9 May 2018

Academic Editor: Hana Vaisocherova-Lisalova

Alzheimer's disease (AD) is a neurodegenerative disease, which affects millions of people worldwide. Curing this disease has not gained much success so far. Exhaled breath gas analysis offers an inexpensive, noninvasive, and immediate method for detecting a large number of diseases, including AD. In this paper, a new method is proposed to detect butylated hydroxytoluene (BHT) in the air, which is one of the chemicals found in the breath print of AD patients. A three-layer sensor was formed through deposition of a thin layer of graphene onto a glassy carbon substrate. Selective binding of the analyte was facilitated by electrochemically initiated polymerization of a solution containing the desired target molecule. Subsequent polymerization and removal of the analyte yielded a layer of polypyrrole, a conductive polymer, on top of the sensor containing molecularly imprinted cavities selective for the target molecule. Two sets of sensors have been developed. First, the graphene sensor has been fabricated with a layer of reduced graphene oxide (RGO) and tested over 5–100 part per million (ppm). For the second batch, Prussian blue was added to graphene before polymerization, mainly for enhancing the electrochemical properties. The sensor was tested over 0.02-1 parts per billion (ppb) level of concentration while the sensor resistance has been monitored.

1. Introduction

Alzheimer's disease (AD) is the sixth cause of death in the USA. In 2016, the cost of AD was evaluated as 236 billion dollars [1]. It is known by a decline in memory, language, problem solving, reasoning, planning, and other thinking and cognitive skills. It happens when the neurons in the brain are damaged or destroyed, so data process and transmission in the brain will be spoiled. Later, by spreading the disease in the brain, the patient will not be able to perform daily activities such as walking or eating [1]. The diagnosis procedures usually take so long. It starts with the evaluation of patient's cognitive ability and reviewing medical history. It continues with lab tests and imaging techniques to visualize the damaged brain tissue [1]. When the damaged tissue is clearly observed by MRI and CT, it is too late to cure the disease since the patient has already lost part of the brain tissues. Researchers have shown that AD starts years, if not decades, before it is diagnosed [2]. The sooner the disease can be diagnosed, the better treatment options can be provided.

Amyloid beta (Aβ) is a peptide known as the biomarker of AD. Aggregation of Aβ in the brain is thought to initiate neurotoxic phenomenon, including neuron inflammation and synaptic and neuronal loss [3]. Destroying the already developed and/or stopping the development of Aβ in the brain are the best options [4, 5], but it has not gained much success. Some researchers tried to detect Aβ in cerebrospinal fluid (CSF), blood, and exhaled breath and correlate it with AD. It has been shown that Aβ is existed in CSF and in less concentration in blood of AD patients [6, 7]. Bach et al. [8] tried to detect Aβ in the exhaled breath with enzyme-linked

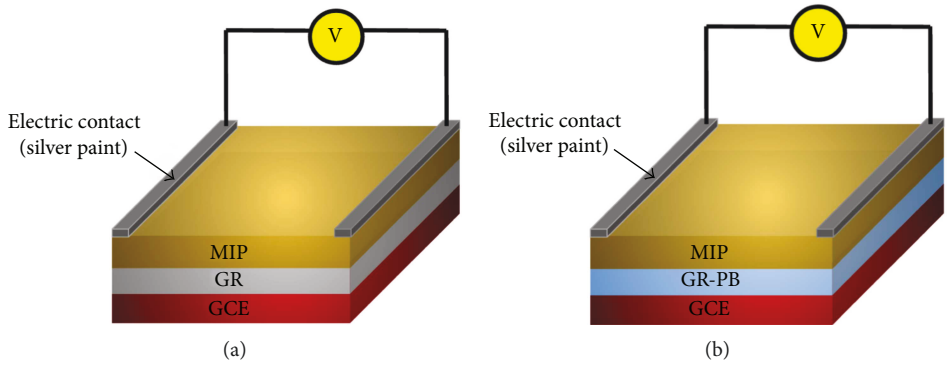

Figure 1: The schematic diagram of both sensors is shown. A layer of molecular imprinting polymer (MIP) is deposited on graphene (GR) or graphene-Prussian blue (Gr-PB) modified surface of the glassy carbon electrode (GCE).

immunosorbent assay (ELISA). However, they found a higher level of Aβ in the healthy control's breath. Besides, researchers found a relationship between Aβ with narcolepsy, a sleep disorder. They detected lower CSF Aβ_{42} levels in the whole narcolepsy group with respect to controls [9].

It was first found by Greek scientists that human breath provides clues into the physiological status of the body [10]. Human breath is mainly composed of nitrogen, oxygen, carbon dioxide, and hydrogen [11]. VOCs are organic chemicals with high vapor pressure (at room temperature), that, along with inert gases, forms less than 1% of the exhaled breath. From the physiological point of view, the exchange of blood and the air in the alveolar leads to transferring chemicals in the blood, which was formed during metabolism inside the body, to find a way to the exhaled breath. Thus, measurement of VOCs in the breath can provide a window into the biochemical processes of the body. A growing number of studies tried to demonstrate the correlation of VOCs and neurodegenerative diseases, including AD and PD [12]. Using gas chromatography and mass spectroscopy and comparing the breath print of the healthy people to AD patients, the list of additional chemicals was found [13, 14]. Butylated hydroxytoluene (BHT) was listed as the chemical found in the breath print of AD and PD patients [15]. BHT is an aromatic benzene ring derivation that is known for its antioxidant properties. In this paper, we report fabrication and testing of two sets of the electrochemical gas sensor, which can sense butylated hydroxytoluene in the air. The proposed sensors are composed of three layers: glassy carbon electrode (GCE); graphene (GR) or graphene-Prussia blue (GR-PB); and molecular imprinting polymer (MIP). Figure 1 shows the schematic diagram of both sensors.

Glassy carbon is an advanced material of pure carbon combining glassy and ceramic properties. Its high purity, extreme corrosion resistance, impermeability to gas and liquid, high strength, high-temperature resistance, low oxidation rate, and high chemical inertness make it suitable to be used frequently as electrode [16, 17]. Graphene is a 2D material known for its unique electrochemical and structural properties. One atom thick graphene has high thermal and electrical conductivity, chemical stability, high specific surface area, and excellent room temperature carrier mobility.

Table 1: Comparison of the Prussian blue sensors for sensing purposes [21].

Modified electrode	Range of detection	Limit of detection
Prussian blue	0.32–5.3 μM	0.018 μM
Copper-iron hexacyanoferrates	0.3–300 μM	0.05 μM
Graphene oxide/Prussian blue	0.02–0.2 mM	1.9 μM
Graphene oxide/Prussian blue	10–1440 μM	3 μM
Polyelectrolyte-functionalized ionic liquid decorated graphene sheets	5–60 μM	1 μM
Gold-Prussian blue-graphene	0.01–3.0 mM	1.5 μM
Prussian blue/reduced graphene oxide	0.5–400 μM	0.44 μM
Reduced graphene oxide/Prussian blue	0.8–500 μM	0.25 μM

These peculiar properties have highlighted the potential of applying this material in a variety of applications, such as electronics, sensors, catalysis, energy-storage devices, and drug delivery. Its two-dimensional nature leads to a high affinity between graphene and the MIP components and makes it suitable for electron transfer between the two layers. The gas-sensing mechanism of graphene is generally described as electron donors or acceptors. This causes a change in the conductance of graphene. So layers of GR have been used to modify the surface of the electrode to improve the electron transfer [18, 19]. Prussian blue (PB, ferric ferrocyanide), formula Fe_4 $[Fe(CN)_6]_3$, is a microcrystalline blue powder. It is an inorganic conductive material that exhibits high electrocatalytic activity and improves the electrochemical sensitivity [20]. It has been extensively studied for its attractive electrochemical properties and wide applications in the field of sensors. In many cases, PB has been used as a mediator with graphene. Combination of GR and PB lead to a synergistic effect that can help the electron transfer [21].

Cyanide ion is very stable at room temperature, and the concentration of free Fe^{+2} ions is negligible. However, in acidic media (pH = 1.7), Fe^{+2} will release from cyanide and it is then oxidized to Fe^{+3}. The released electrons together with H^+ would react with oxygen-containing groups on GO, leading to the partial reduction of GO to rGO at room temperature. In the meantime, Fe^{+3} ions interacted with

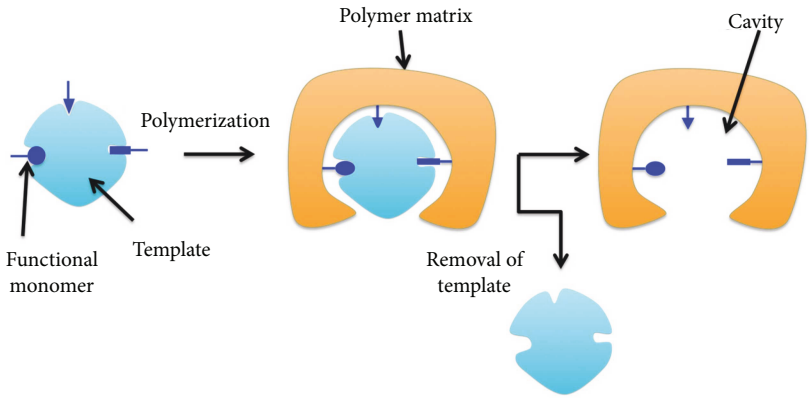

Figure 2: Molecular imprinting technology: template molecule is placed in the polymer along with functional monomers and cross-linkers. By applying voltage, polymerization starts. After the polymerization, a washing agent removes the template molecules. So cavities, which can only trap the same size and shape of the template, are left behind.

carboxyl groups of GO and confined on the surface of GO. With the existence of cyanide, they form PB cubes [22]. At the pH 1.7, the acid is not strong enough to form cyanide acid, but for precautions, it is recommended to do the procedures under the hood, respirator, and so on.

Table 1 summarizes the PB-GR sensors, which were used for sensing purposes and include the range and limit of detection [21].

Molecular imprinting is a technique to polymerize around a template molecule and remove the template after polymerization. It leaves cavities with the exact size and shape of the template in the polymer matrix [23]. Three key elements in molecular imprinting technique are the target molecule (or template), which is what is being sensed; the functional monomer which is a compound having chemical and shape complementarity to the template and will help the polymerization to form the polymer matrix; and the cross-linking agent (or cross-linker) that is a multifunctional molecule containing two or more reactive split ends able to interact via chemical bound [24]. The size and shape of the cavity allow the target molecule or similar molecules to occupy the cavity, but the functional monomer orientation just allows binding with the template molecule [23]. Figure 2 represents the MIP process.

Besides the size, shape, and orientation of functional monomers, the selectivity of MIP to the target molecule is performed by the covalent or noncovalent bonding happens between the template molecule and the polymer matrix [25–27]. In this case, hydrogen bonding between the BHT molecules and the polymer polypyrrole is formed. Molecular imprinting enables the creation of stable and selective "artificial receptors." It utilizes associative self-assembly between target analytes and material precursors to create a molecular "lock and key" architecture within an electrochemical sensor for ultrasensitive and selective detection. MIPs are also cost-effective, robust, long-term stable, and are able to self-recover. Selectivity of MIP has been reported frequently. Dickert et al. [28] reported that MIP could recognize molecular shapes: the lean toluene is favored by factor of six to the more bulky o-xylene; even the three xylenes can be distinguished from each other.

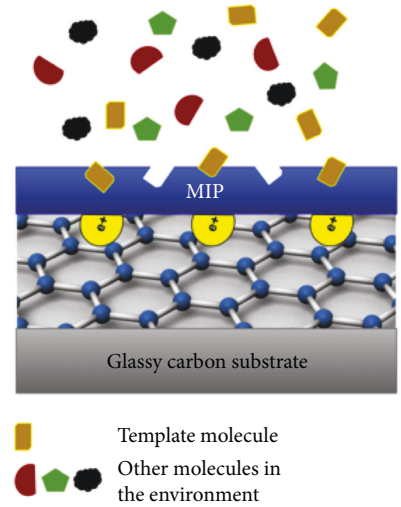

Figure 3: The mechanism of the sensor is depicted. Among different molecules in the environment, only the template molecule can be absorbed in the molecular imprinting polymer (MIP) layer. When the template molecule is trapped in the MIP layer, an extra electron is transferred to the graphene layer, which will cause resistance change.

Examples of common sensors for chemical sensing include surface acoustic waves (SAWs), quartz microbalance (QMB), and gold nanoparticles. SAW is elastic waves propagating along the surface of an elastic substrate, whose amplitudes decay exponentially with the substrate depth. The change in gas concentration results in a change in the mass and leads to an electrical conductivity shift of the chemical interface. These changes influence the SAW amplitude and the phase velocity [29]. These sensors need a concentration calibration. Besides, the sensor response is not instant. In QMB sensors, a slight mass change on the quartz surface results in a frequency change of the electrical output signal of the oscillator circuit, at which each sensor is connected [30]. The problem with QMB sensors is that the molecules with the same mass can confuse the sensor and make the same resonance frequency. Besides, the retention

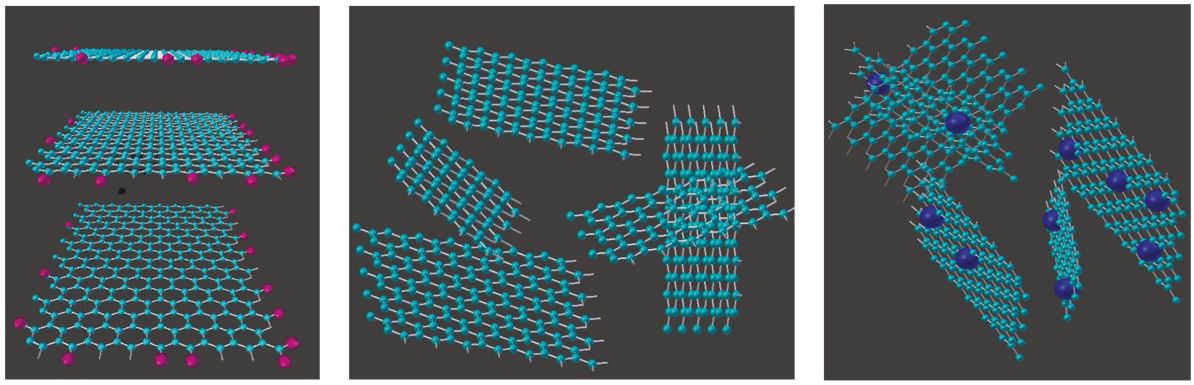

(a) (b) (c)

Figure 4: Transformation of graphene oxide to reduced graphene oxide-Prussian blue. (a) Stack of graphene oxide. (b) Randomly oriented layers of reduced graphene oxide after reduction. (c) Preparation of Prussian blue on reduced graphene oxide layers.

time can take up to several minutes and the sensitivity of the sensor is poor. Functionalized gold nanoparticles (GNPs) on field effective transistor are an electrical device that can act as a switch or can sense the gate resistance by applying an electric field to the source and the drain. It has been used to detect chemicals by adding reactant elements on the gate that can absorb the desired chemical [31]. However, the problem with FET sensors is that it cannot absorb large chemicals. Besides, different molecules with the same reactant can mislead the sensor. MIP sensors compared to the similar ones have huge advantages, as the molecules with the same mass or chemical properties cannot mislead the sensors, they sense instantly and they can sense a variety of molecules from small to very large. This type of sensor includes a sensing circuit configured to detect and report resistance change in the layer of MIP. The binding of the target molecules causes the resistance change to the MIP. The sensing mechanism of this sensor has been depicted in Figure 3.

2. Materials and Methods

Two sets of electrochemical sensors were fabricated. The fabrication steps are the same, except that for the GR-PB sensor, additional steps for preparation of PB are needed. The materials and equipment are listed below:

2.1. Chemical and Equipment. Glassy carbon plate was purchased from Alfa Aesar (MA, USA). Hydrazine hydrate, phosphate buffer solution, pyrrole, graphene oxide, and butylated hydroxytoluene were obtained from Sigma-Aldrich (MO, USA). All the solutions were prepared with deionized (DI) water.

Potentiostat model Solartron SI 1287 was used to conduce the cyclic voltammetry. The potentiostat potential range was from −14.5 V to 14.5 V, and the sweep rate was from 6 mV/min to 6000 V/min. Electrochemical measurements were carried out with a three-electrode system consisting of a platinum wire as the auxiliary electrode, a KCl saturated Ag/AgCl reference electrode, and modified glassy carbon as the working electrode. Ultrasonicator XL 2120 and centrifuge Legend X1R were used for homogenizing and distillation of

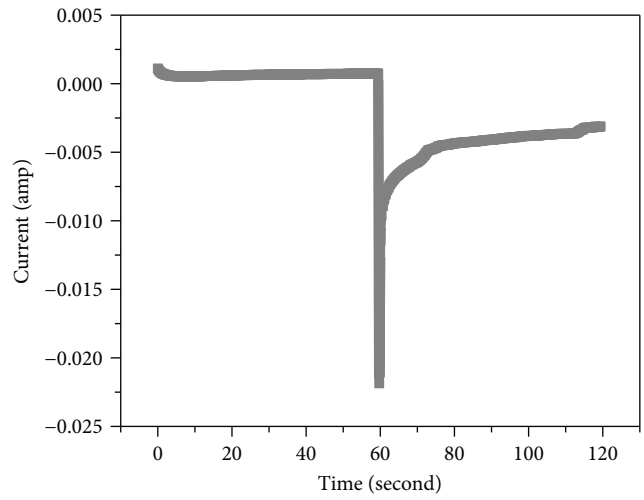

Figure 5: Activation process of the glassy carbon electrode (GCE), which is the same for both sensors, is shown. Before use, a constant voltage −1.6 and 1.6 V was applied to the GCE, each for 60 seconds.

the graphene solution. The spectroscopy was done with Raman Horiba HR800.

2.2. Graphene Synthesize. Reduced graphene oxide (RGO) was synthesized from graphene oxide (GO) based on Hummer method [32–35]. In brief, the GO (500 mg) was dispersed in deionized water (500 mL) followed by ultrasonication. After that, 2 mL of hydrazine hydrate was added to the above dispersion. The obtained solution was stirred at 100°C for 24 h [23]; the resulting mirror-like graphene dispersion was filtered with 0.22 μm pore size filter and washed with deionized water several times. Finally, a gray layer was obtained. Figures 4(a) and 4(b) show the procedure of obtaining reduced graphene oxide from graphene oxide.

2.3. GR-PB Preparation. Preparation of PB was according to the literature [22, 36]. First, 2 mg of the produced GR was added to 2 mL of deionized water and ultrasonicated to obtain a homogenous black solution. The solution

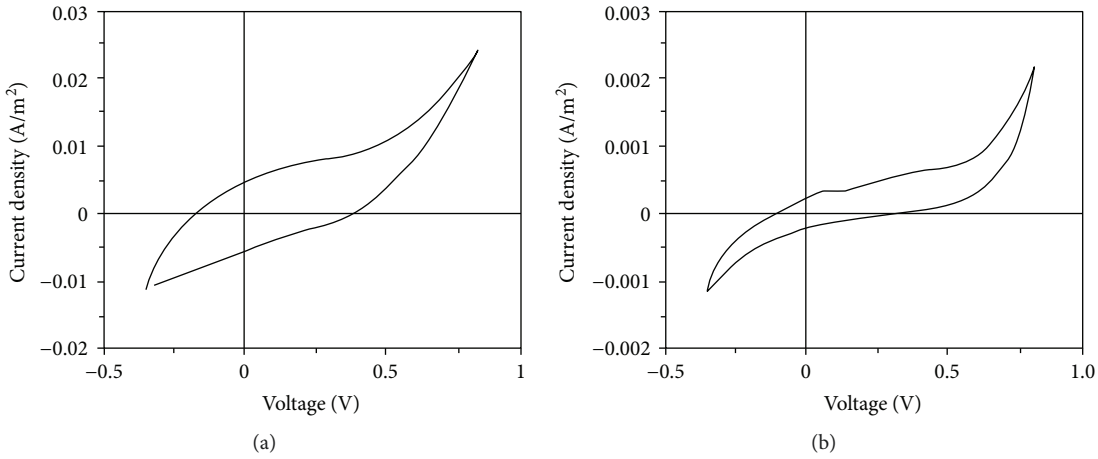

Figure 6: The last cycle of cyclic voltammetry (polymerization process) of the graphene sensor (a) and the graphene-Prussian blue sensor (b) is shown. The voltage range of −0.35 to 0.85 V was applied.

was then added into 5 mL of an aqueous solution containing 0.006 g $FeCl_3$.6H2O, 0.008 g $K_3Fe(CN)_6$, and 0.037 g KCl (pH adjusted to 1.5 with HCl) by stirring at room temperature for 12 hours. The product was then centrifuged (2000 rpm for 20 min) and washed with the DI water several times and dried overnight under a vacuum condition at 40°C. Figure 4 depicts the procedures for obtaining GR-PB from GO.

2.4. Fabrication of MIP. The glassy carbon electrode (GCE) was washed and then activated by applying a pulse voltage +1.6 and −1.6 V versus Ag/AgCl for 60 seconds each [23, 37]. The response in current is shown in Figure 5. The activation process was done in phosphate buffer solution (pH 6.8) using a three-electrode system, with the glassy carbon electrode as the working, Ag/AgCl as the reference, and platinum as the auxiliary electrode. A large current response occurs when the potential changes to −1.6 V indicative of a reductive process of the GCE. Then, it was left to dry overnight.

The GCE surface was modified by adding 2 mg of the GR-PB powder dissolved in 2 mL of DI water. It was stored overnight. A solution of 1 L phosphate buffer solution containing 0.09 BHT and 6.937 mL of pyrrole was stirred for 2 h (pH 6.8, adjusted with HCl) to be used for cyclic voltammetry (CV). The cyclic voltammetry to deposit the polymer was carried out for 20 cycles with a scan rate of 50 mV/s, from −0.35 to +0.85 V versus Ag/AgCl. The resulting CVs are shown in Figure 6. The CV without PB is highly capacitive. After the polymerization process, the sensor was washed with ethanol and left to dry overnight.

3. Results

3.1. Graphene Characteristic. Raman spectroscopy is often used in chemistry to provide a structural fingerprint by which molecules can be identified. It has been applied to identify the produced RGO structure. Figure 7 shows the results.

From Raman analyst, the D band is strong, which indicates the graphene has some defect. The full width at half maximum of the 2D band is about 80, and the intensity ratio

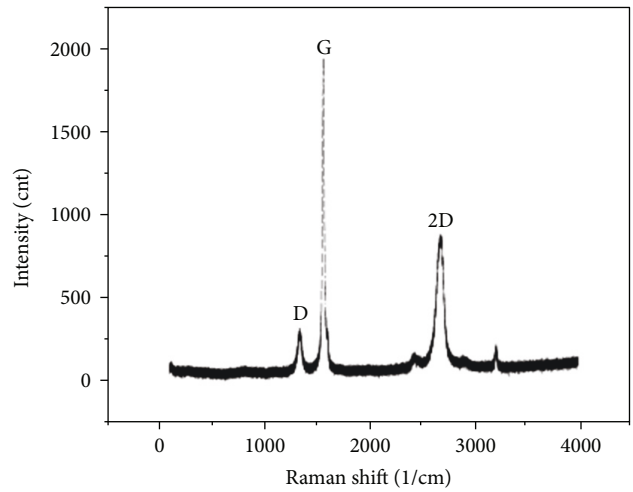

Figure 7: The reduced graphene oxide (RGO) was tested by Raman spectroscopy. It was derived that RGO is multilayers between 6 and 10.

of G/2D is more than 1, which shows that the graphene should be multilayer graphene, between 6 and 10 layers.

3.2. Testing Chamber. A sealed chamber was fabricated for the gas testing. It was made of polycarbonate 0.5-inch thick and the volume of the chamber was almost 0.5 m^3. The solid vapor pressure of BHT was simulated with ASPEN software. Based on the software results, a specific amount of solid BHT was left inside a syringe to evaporate. The vapor was then injected into the chamber and the sensor was given time to reach to steady state before reading the resistance.

3.3. SEM Images. SEM images have been taken after removal of the templates for both sensors. The lighter color molecules on the top represent the MIP molecules. These images clearly show that GR-PB sensor has a more porous surface on top compared to GR sensor, which can lead to absorbing more template molecules. Figure 8 shows the SEM images of GR and GR-PB sensors. Furthermore, the GR-PB sensor has a

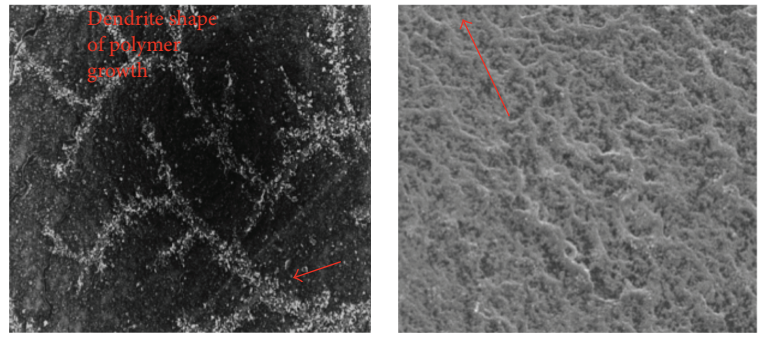

Figure 8: SEM images of the GR sensor with dendrite shape of polymer growth (a) and the image of the GR-PB sensor (b) are shown. Prussian blue caused the polymer to form in more directions.

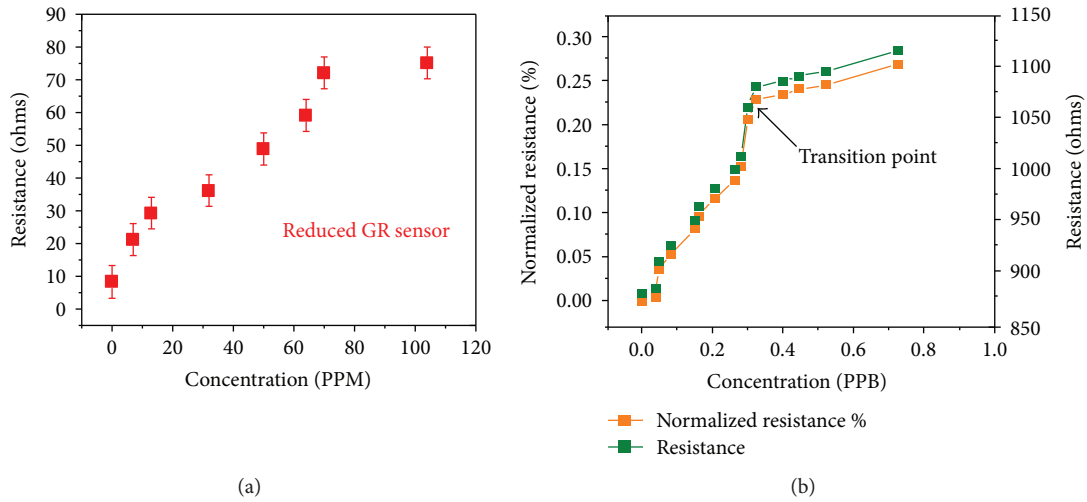

Figure 9: Testing results of the GR sensors in the range of 5–100 ppm in red and the GR-PB sensor in the range of 0.02 to 1 ppb in green along with the normalized resistance change are shown. At 0.3 ppb concentrations, the vacuum was purged to the sealed chamber, so the resistance increase happens with a slower slope.

surface of more uniform and that is because of the presence of PB.

3.4. Testing Results. The GR sensor was tested in the range of 5 to 100 ppm, and the GR-PB sensor was tested over the range of 0.02 to 1 ppb. For each measurement, a syringe of a specific vapor of BHT was injected into the chamber and it was left to reach equilibrium, while the resistance was monitored. Both sensors have almost linear behavior. The results show that Prussian blue has a huge impact on the limit of detection of the sensor. Furthermore, PB increased the sensor resistance (in the absence of any chemical), which made it easier to monitor in case of a small resistance change. The results are shown in Figure 9. In the middle of the GR-PB sensor testing, the vacuum was purged into the chamber and it slowed down the resistance change. Normalized resistance was calculated based on $[(R - R_0)/R_0] \times 100$.

Figure 10 shows the behavior of the sensor at the time of exposure. One-tenth mole of solid BHT is placed inside the sealed chamber, while the resistance was monitored. After one minute, the solid BHT was removed from the chamber

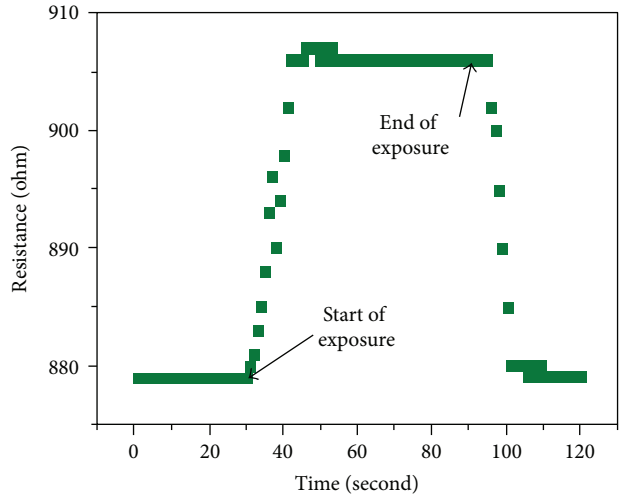

Figure 10: The behavior of the sensor at the time of exposure is shown. Between 0 and 30 seconds, the sensor is resting. At the time $t = 30$ s, the sensor is exposed to BHT and $t = 70$ s is the end of exposure.

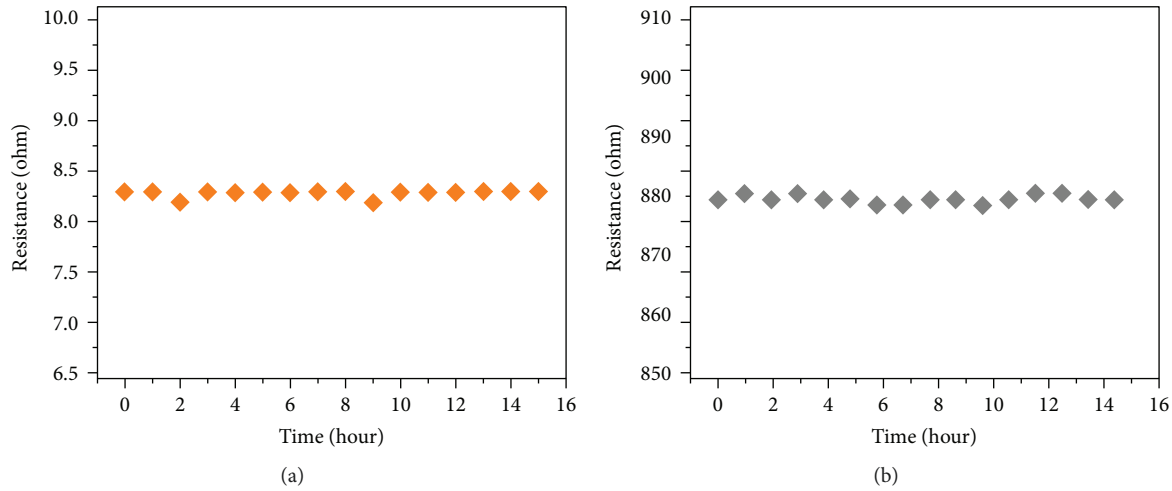

Figure 11: Stability test for the graphene sensor (a) and the graphene-Prussian blue sensor (b) are shown. The resistance of both sensors was monitored for fifteen hours in the absence of the BHT.

and as shown, it took a few seconds for the sensor to remain back to its resting resistance. The vapor pressure of 0.1 mole BHT inside the chamber was 500 ppb; however, the time is so limited so it could not reach the equilibrium.

Before starting the test, the stability of both sensors was evaluated. The resistance of the sensors was monitored for 15 hours inside the sealed chamber in the absence of the BHT. A negligible change was observed for both sensors during the monitoring time. So the authors concluded that both sensors are stable. The results are shown in Figure 11.

4. Discussion

Both sensors have been tested for sensitivity toward water vapor and nitrogen since these are the two main components of the exhaled breath. Pure nitrogen has been pumped to the sealed chamber and the sensors' response was monitored for 10 minutes. The same experiment was done for water vapor. A beaker of 300 ml boiling water with a heater was placed inside the chamber, while the resistance was monitored for 10 minutes. Since no changes in the resistance were observed, so it can be suggested that the sensors were not sensitive to nitrogen or water vapor.

The proposed PB-GR sensor is super sensitive as its limit of detection is 0.02 ppb. It is the most sensitive sensor reported so far. The concentrations of VOCs reported in the AD patients print are in the range of 1–20 ppb [15], so our proposed GR-PB sensor is capable of sensing the BHT in the exhaled breath of AD patients. These gas sensors are very selective and similar molecules cannot mislead them. The fabrication steps are straightforward and can be done in a week. These low-cost sensors can be used repeatedly after being washed with ethanol.

5. Conclusions

Two electrochemical sensors have been fabricated to sense BHT in the air at ppm and ppb levels. The graphene sensor was tested at ppm level and the graphene-Prussian blue sensor was tested at ppb level. BHT was detected at a very low concentration, less than 20 ppb, the target range for sensing it in the exhaled breath of Alzheimer's patients. The developed electrochemical sensors exhibited excellent performance such as a low limit of detection, wide range of detection, high selectivity, good stability, and easy reproducibility toward sensing BHT. The SEM imaging showed that the GR-PB modified sensor had more porous structure than the GR-modified sensor. Besides, the testing results proved that adding PB to graphene would increase the limit of detection. It is actually because the PB exhibits high electrocatalytic activity and thus improves the electrochemical sensitivity of the sensor. The high affinity between GR and PB will increase the electron transfer between the layers. In the future, this sensor can be used as an array to detect all the chemicals found in the exhaled breath of AD patients.

Disclosure

An earlier version of this work was presented at "RISE: 2017 | Research, Innovation, and Scholarship Expo," and "2017 A meeting of Materials Research Society (MRS)."

Conflicts of Interest

The authors declare no conflict of interest.

References

[1] Alzheimer's Association, "2016 Alzheimer's disease facts and figures," *Alzheimer's & Dementia*, vol. 12, no. 4, pp. 459–509, 2016.

[2] G. De Meyer, F. Shapiro, and H. Vanderstichele, "Diagnosis-independent Alzheimer disease biomarker signature in cognitively normal elderly people," *Archives of Neurology*, vol. 67, no. 8, pp. 949–956, 2010.

[3] D. J. Selkoe, T. Yamazaki, M. Citron et al., "The role of APP processing and trafficking pathways in the formation of amyloid β-protein," *Annals of the New York Academy of Sciences*, vol. 777, no. 1, pp. 57–64, 1996.

[4] F. H. Iaccarino, C. A. Singer, J. A. Martorell et al., "Gamma frequency entrainment attenuates amyloid load and modifies microglia," *Nature*, vol. 540, no. 7632, pp. 230–235, 2016.

[5] R. G. Canter, J. Penney, and L. Tsai, "The road to restoring neural circuits for the treatment of Alzheimer's disease," *Nature*, vol. 539, no. 7628, pp. 187–196, 2016.

[6] J. L. Urraca, C. S. A. Aureliano, E. Schillinger, H. Esselmann, J. Wiltfang, and B. Sellergren, "Polymeric complements to the Alzheimer's disease biomarker β-amyloid isoforms Aβ1–40 and Aβ1–42 for blood serum analysis under denaturing conditions," *Journal of the American Chemical Society*, vol. 133, no. 24, pp. 9220–9223, 2011.

[7] W. T. Hu, A. Chen-Plotkin, S. E. Arnold et al., "Biomarker discovery for Alzheimer's disease, frontotemporal lobar degeneration, and Parkinson's disease," *Acta Neuropathologica*, vol. 120, no. 3, pp. 385–399, 2010.

[8] J. P. Bach, M. Gold, D. Mengel et al., "Measuring compounds in exhaled air to detect Alzheimer's disease and Parkinson's disease," *PLoS One*, vol. 10, no. 7, article e0132227, 2015.

[9] C. Liguori1, F. Placidi, F. Francesca Izzi et al., "Beta-amyloid and phosphorylated tau metabolism changes in narcolepsy over time," *Sleep and Breathing*, vol. 20, no. 1, pp. 277–283, 2016.

[10] B. Buszewski, M. Kesy, T. Ligor, and A. Amann, "Human exhaled air analytics: biomarkers of diseases," *Biomedical Chromatography*, vol. 21, no. 6, pp. 553–566, 2007.

[11] T. Hibbard and A. J. Killard, "Breath ammonia analysis: clinical application and measurement," *Critical Reviews in Analytical Chemistry*, vol. 41, no. 1, pp. 21–35, 2011.

[12] M. K. Nakhleh, H. Amal, R. Jeries et al., "Diagnosis and classification of 17 diseases from 1404 subjects via pattern analysis of exhaled molecules," *ACS Nano*, vol. 11, no. 1, pp. 112–125, 2017.

[13] A. Mazzatentaa, M. Pokorskide, F. Sartuccib, L. Domenicib, and C. D. Giulioa, "Volatile organic compounds (VOCs) fingerprint of Alzheimer's disease," *Respiratory Physiology & Neurobiology*, vol. 209, pp. 81–84, 2015.

[14] U. Tisch, I. Schlesinger, R. Ionescu, M. Nassar, N. Axelrod, and D. Robertman, "Detection of Alzheimer's and Parkinson's disease from exhaled breath using nanomaterial-based sensors," *Nanomedicine*, vol. 8, no. 1, pp. 43–56, 2013.

[15] Y. Y. Broza and H. Haick, "Nanomaterial-based sensors for detection of disease by volatile organic compounds," *Nanomedicine*, vol. 8, no. 5, pp. 785–806, 2013.

[16] A. Dekanskia, J. Stevanovic, R. Stevanovic, B. Z. Nikolic, and V. M. Jovanovic, "Glassy carbon electrodes: I. Characterization and electrochemical activation," *Carbon*, vol. 39, no. 8, pp. 1195–1205, 2001.

[17] W. E. Van der Linden and J. W. Dieker, "Glassy carbon as electrode material in electro- analytical chemistry," *Analytica Chimica Acta*, vol. 119, no. 1, pp. 1–24, 1980.

[18] F. Schedin, A. K. Geim, S. V. Morozov et al., "Detection of individual gas molecules adsorbed on graphene," *Nature Materials*, vol. 6, no. 9, pp. 652–655, 2007.

[19] T. Alizadeh and L. Hamedsoltani, "Graphene/graphite/molecularly imprinted polymer nanocomposite as the highly selective gas sensor for nitrobenzene vapor recognition," *Journal of Environmental Chemical Engineering*, vol. 2, no. 3, pp. 1514–1526, 2014.

[20] J. Zhao, G. Chen, L. Zhu, and G. Li, "Graphene quantum dots-based platform for the fabrication of electrochemical biosensors," *Electrochemistry Communications*, vol. 13, no. 1, pp. 31–33, 2011.

[21] J. Li, Y. Jiang, Y. Zhai, H. Liu, and L. Li, "Prussian Blue/reduced graphene oxide composite for the amperometric determination of dopamine and hydrogen peroxide," *Analytical Letters*, vol. 48, no. 17, pp. 2786–2798, 2015.

[22] M. Zhang, C. Hou, A. Halder, J. Ulstrup, and Q. Chi, "Interlocked graphene–*Prussian blue* hybrid composites enable multifunctional electrochemical applications," *Biosensors and Bioelectronics*, vol. 89, Part 1, pp. 570–577, 2017.

[23] Y. X. Li, Y. J. Li, H. Mei et al., "Highly sensitive protein molecularly imprinted electro-chemical sensor based on gold microdendrites electrode and prussian blue mediatedamplification," *Biosensors and Bioelectronics*, vol. 42, pp. 612–617, 2013.

[24] M. Cui, S. Liu, W. Lian, J. Li, W. Xua, and J. Huang, "A molecularly-imprinted electrochemical sensor based on a graphene–Prussian blue composite-modified glassy carbon electrode for the detection of butylated hydroxyanisole in foodstuffs," *Analyst*, vol. 138, no. 20, pp. 5949–5955, 2013.

[25] D. S. Janiak and P. Kofinas, "Molecular imprinting of peptides and proteins in aqueous media," *Analytical and Bioanalytical Chemistry*, vol. 389, no. 2, pp. 399–404, 2007.

[26] C. Algieri, E. Drioli, L. Guzzo, and L. Donato, "Bio-mimetic sensors based on molecularly imprinted membranes," *Sensors*, vol. 14, no. 8, pp. 13863–13912, 2014.

[27] G. Vasapollo, R. Del Sole, L. Mergola et al., "Molecularly imprinted polymers: present and future prospective," *International Journal of Molecular Sciences*, vol. 12, no. 9, pp. 5908–5945, 2011.

[28] F. L. Dickert, P. Leiberzeit, S. G. Miarecha, K. J. Mann, O. Hayden, and C. Palfinger, "Synthetic receptors for chemical sensors—subnano- and micrometre patterning by imprinting techniques," *Biosensors and Bioelectronics*, vol. 20, no. 6, pp. 1040–1044, 2004.

[29] X. Chen, M. Cao, Y. Li et al., "A study of an electronic nose for detection of lung cancer based on a virtual SAW gas sensors array and imaging recognition method," *Measurement Science and Technology*, vol. 16, no. 8, pp. 1535–1546, 2005.

[30] R. Capuano, M. Santonico, G. Pennazza et al., "The lung cancer breath signature: a comparative analysis of exhaled breath and air sampled from inside the lungs," *Scientific Reports*, vol. 5, no. 1, article 16491, 2015.

[31] Y. Ma and A. Siitonen, "Chemical sensor using molecularly-imprinted single layer graphene," Patent no: US 20160377611 A1, 2016.

[32] W. S. Hummers and R. E. Offeman, "Preparation of graphene oxide," *Journal of the American Chemical Society*, vol. 80, no. 6, article 1339, 1958.

[33] S. Stankovich, D. A. Dikin, R. D. Piner et al., "Synthesis of graphene-based nanosheets via chemical reduction of exfoliated graphite oxide," *Carbon*, vol. 45, no. 7, pp. 1558–1565, 2007.

[34] S. Park, J. An, J. R. Potts, A. Velamakanni, S. Murali, and R. S. Ruoff, "Hydrazine-reduction of graphite- and graphene oxide," *Carbon*, vol. 49, no. 9, pp. 3019–3023, 2011.

[35] S. Pei and H. Cheng, "The reduction of graphene oxide," *Carbon*, vol. 50, no. 9, pp. 3210–3228, 2012.

[36] E. Jin, X. Lu, L. Cui, D. Chao, and C. Wang, "Fabrication of graphene/prussian blue composite nanosheets and their electrocatalytic reduction of H_2O_2," *Electrochimica Acta*, vol. 55, no. 24, pp. 7230–7234, 2010.

[37] A. Ping, J. F, J. Wu, K. Fan, and Y. B. Ying, "An amperometric sensor based on Prussian blue and poly(*o*-phenylenediamine) modified glassy carbon electrode for the determination of hydrogen peroxide in beverages," *Food Chemistry*, vol. 126, no. 4, pp. 2005–2009, 2011.